

An Efficient Test-Time Scaling Approach for Image Generation

Vignesh Sundaresha
UIUC
vs49@illinois.edu

Akash Haridas
AMD
akash.haridas@amd.com

Vikram Appia
AMD
vikram.appia@amd.com

Lav Varshney
Stony Brook University
lav.varshney@stonybrook.edu

Abstract

Image generation has emerged as a mainstream application of large generative AI models. Just as test-time compute and reasoning have helped language models improve their capabilities, similar benefits have also been observed with image generation models. In particular, searching over noise samples for diffusion and flow models has shown to scale well with test-time compute. While recent works have explored allocating non-uniform inference-compute budgets across different denoising steps, they rely on greedy algorithms and allocate the compute budget ineffectively. In this work, we study this problem and propose solutions to fix it. We propose the Verifier-Threshold method which automatically reallocates test-time compute and delivers substantial efficiency improvements. For the same performance on the GenEval benchmark, we achieve a $2\text{-}4\times$ reduction in computational time over the state-of-the-art method.

1 Introduction

Image generation using AI has become a popular application with several models [5, 6, 7, 8, 9] being widely used. However, even state-of-the-art models often struggle to accurately follow detailed prompt instructions [1, 10]. To address this limitation, the vision community has drawn inspiration from the language domain by incorporating test-time compute [11] and reasoning [12], leading to the development of analogous approaches for vision tasks [13, 14]. However, reasoning-based methods inherently demand computational power and time during inference, which becomes costly at large scales [15] or on resource-constrained devices [16]. Consequently, improving the efficiency of these test-time compute algorithms becomes essential.

Fig. 1 illustrates how test-time scaling substantially increases computational requirements. The baseline implementation [4] requires between $3\times$ and $10\times$ more compute time over regular image generation to achieve performance gains of 8% to 12% respectively on GenEval [1]. In contrast, our proposed method, *Verifier-Threshold*, reaches the same 12% improvement using just $(1/4)^{\text{th}}$ of the computational cost of

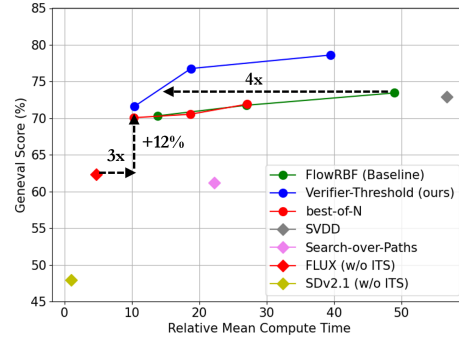


Figure 1: Test-time scaling; the horizontal axis represents relative wall clock duration on an AMD MI300X GPU averaged across 553 GenEval [1] prompts and the vertical axis represents the Overall GenEval score. VQAScore [2] is used as verifier and FLUX-Schnell [3] as generator for all methods. The *Verifier-Threshold* method is consistently more efficient and delivers higher scores compared to the baseline FlowRBF [4] as well as other methods.

the baseline, clearly demonstrating its efficiency. Furthermore, our algorithm continues to benefit from scaling, achieving gains of up to 15%.

The key contributions of this work are twofold: *identifying the “compute-dumping” issue* in the existing baseline algorithm and *introducing the “Verifier-Threshold” algorithm* as a solution. We validate our approach on state-of-the-art image generation models and datasets. We organize the rest of the paper as follows: Sec. 2 discusses the baseline algorithm and experimental setup. Sec. 3 shows the compute dumping phenomenon and possible solutions, including our proposed Verifier-Threshold approach. Lastly, Sec. 4 presents results, including some example images generated by the different approaches.

2 Preliminaries

2.1 Test-time Scaling and FlowRBF

Diffusion models [17, 18] and flow models [3] along with autoregressive models [19] have become the mainstream methods for image generation. Test-time scaling for image generation basically aims to use the compute available at test-time to improve performance, either through increasing the denoising steps [20] or searching for better noises [13, 4]. Noise-search in particular has shown to scale much better than denoising steps [13]; hence we focus on that here. FlowRBF [4] proposes a key idea of *non-uniform inference-compute budget allocation across denoising steps* which is a crucial advance in noise-search approaches. Using this idea, it beats all previous baseline methods such as Best-of- N (which performs as good as zero-order and Search-over-Paths) from [13]. Hence we use FlowRBF [4] as our main baseline, and show improvements on the same flow models as proof-of-concept. However, FlowRBF’s approach of non-uniform allocation and our proposed algorithm can be easily extended to other diffusion models. Prior works are discussed in detail in Appendix B.

2.2 Experimental Setup

We use the FLUX-Schnell model [3] for all our experiments similar to [4]. We use ImageReward [21] and VQAScore [2] as our verifier reward models to guide the noise-search process. For evaluating the performance of different algorithms, we use the GenEval benchmark [1], which consists of prompts that test for attributes such as color, number, position, etc. and helps determine an objective answer. We calculate the average percentage of correct images across different attributes as our performance metric. For the efficiency metric, we use the average wall clock duration (relative to base SDv2.1) taken for each prompt on a single AMD MI300X GPU. We also use the number of function evaluations (NFEs) to indicate the efficiency of the approach (lower is better). More details are discussed in Appendix A.

3 Verifier Threshold

3.1 Compute Dumping and Manual Budgeting

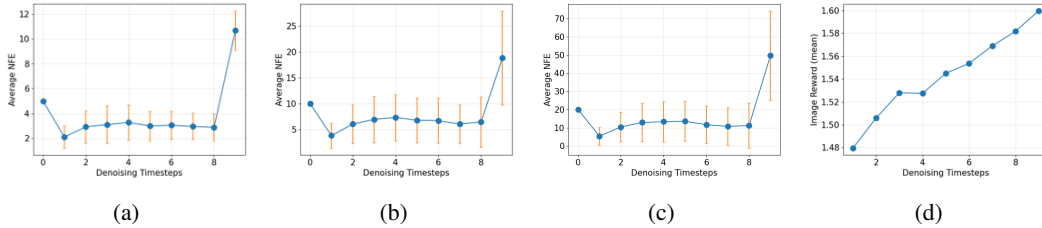


Figure 2: (a), (b) and (c) show how FlowRBF distributes NFEs (or compute budget) across denoising steps, averaged across all GenEval prompts with the total NFE budget set to 40, 80, and 160, respectively. Notice that in all cases, the inference-compute gets “dumped” at the last denoising step, and this issue persists even at total NFE budget as large as 500. (d) shows the verifier score as a function of denoising steps averaged over all GenEval prompts for total NFEs = 80. Notice that the verifier score does not increase at the last step in proportion to the amount of compute dedicated to it, thus wasting the test-time compute budget.

The efficacy of the FlowRBF [4] approach can be mainly attributed to the idea of non-uniform inference-compute allocation across denoising steps or *rollover budget forcing (RBF)*. The basic

concept behind the RBF algorithm is that the denoiser stays in a particular denoising step until either: (a) the verifier score for the new noise particle exceeds the previous step’s highest score, or (b) the per-step maximum compute budget is exhausted. The issue with these criteria is that: (a) it is greedy and jumps to the next step even with a marginally better particle, and (b) it does not account for the “wrong” trajectories the diffusion process takes due to the per-step budget.

Manifestations of these issues are shown in Figs. 2 and 3 where the model performs a ten-step denoising process. Fig. 2 (a, b, c) show that even though the RBF algorithm is designed to allow non-uniform allocation of inference-compute (NFEs), most of the steps (1 to 8) are allocated similar NFEs (except for the zeroth step which is hard-coded to use a pre-defined amount of NFEs). Significant portions of the total test-time NFEs are “dumped” at the last step. When the NFE budget is lower ($=40$) (Fig. 2 (a)), the algorithm quickly exhausts the per-step budget and moves to the next step. When the NFE budget is higher ($=80, 160$) (Figs. 2 (b & c)), the greediness of the RBF algorithm causes it to quickly move to the next step. In both cases, the algorithm has a large NFE budget remaining which it is forced to “dump” in the final denoising step. Fig. 2 (d) shows that the average verifier score at the last denoising step does not increase in proportion to the allocated compute, thus underscoring the dumping issue. Fig. 3 (a) shows an example prompt that highlights the mistake caused by the compute dumping phenomenon.

Intuitively, the RBF budget allocations in Fig. 2 are sub-optimal since the structural changes necessary to obtain a semantically correct image happens in the initial denoising steps, implying that more test-time budget needs to be allocated there rather than at the end. Manually hard-coding the compute distribution to have more budget at the initial steps is one approach to solving this problem as shown in Fig. 3 (b). Although this approach may yield improvements for certain prompts, it does not generalize well across all prompts. Therefore, an algorithm that automatically redistributes the compute budget is necessary.



Figure 3: (a) shows three images generated at different denoising steps for the prompt “a photo of a bench left of a bear” using FlowRBF [4], with a total of 40 NFEs and ImageReward [21] as the verifier. This example illustrates the compute-dumping issue. The first image (at the second denoising step) captures the correct structure, though the texture remains noisy. However, the second image, produced at the third step, achieves the highest verifier score and is therefore selected, despite placing the bear on top of the bench rather than to the left. Because no additional budget is allocated at earlier steps, the denoising process continues from this incorrect latent, ultimately producing a final image with the bear on top of the bench. (b) demonstrates how this issue could be mitigated by manually reallocating the compute budget through hard-coded NFEs at each step (i.e., manual budgeting).

3.2 Verifier-Threshold Algorithm

Rather than advancing to the next denoising step as soon as a higher-reward noise particle is obtained, we propose waiting until the verifier score surpasses the previous one by a significant margin (i.e., a threshold). In this way, the algorithm progresses only when the score at a given step is sufficiently improved. This mechanism forms the basis of our Verifier-Threshold algorithm, as illustrated in Fig. 4a and detailed in Alg. 1.

4 Results

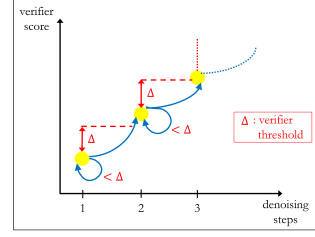
As described in Sec. 2, we evaluate the performance of different algorithms on the GenEval benchmark [1]. Fig. 1 highlights the advantages of our approach when using VQAScore [2] as the verifier. To demonstrate that these benefits generalize across verifiers, we also evaluate performance using ImageReward [21], as shown in Fig. 5. In both cases, our method achieves $2\times$ to $4\times$ higher efficiency for the same benchmark score, or alternatively, a 4% to 5% improvement in benchmark score at the

Algorithm 1 Verifier-Threshold Algorithm

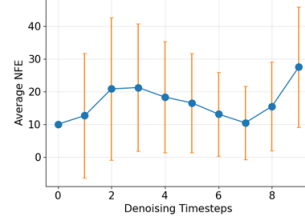
```

1: Input: compute budget  $N$ , denoising timesteps  $T$ ,
   generator model  $\mathcal{G}_\theta$ , verifier model  $\mathcal{R}$ , prompt  $p$ ,
   Verifier-Threshold  $\Delta$ 
2: Output: image
3:  $t = 1$ 
4: for  $n = 1, \dots, N$  do
5:   # sample a noise particle and perform 1 NFE
6:    $\epsilon_n \sim \mathcal{N}(\mathbf{0}, \mathbf{I})$ 
7:    $z_t = \mathcal{G}_\theta(z_{t-1}, \epsilon_n, t, p)$ 
8:   # calculate reward score using verifier
9:    $r_t = \mathcal{R}(\text{Tweedie's}(z_t), p)$ 
10:  # Verifier-Threshold criteria
11:  if  $r_t - r_{t-1} > \Delta$  : then
12:     $t++$ 
13:  end if
14:  if  $t > T$  : then
15:    break
16:  end if
17: end for
18: return Tweedie's ( $z_t$ )

```



(a)



(b)

Figure 4: (a) verifier threshold mechanism and (b) its compute allocation.

same computational cost. All reported results correspond to test-time compute within a practical range of 2–3 minutes. Additionally, Fig. 6 presents example prompts where our algorithm produces objectively correct outputs compared to baseline methods. More comprehensive results and further examples are provided in Appendix C.



(a)



(b)



(c)

Figure 6: The outputs of the model for the prompt “a photo of a wine glass right of a hot dog”. (a), (b), (c) represent the images generated by FLUX-Schnell [3] with no test-time scaling, FlowRBF [4], and Verifier-Threshold, respectively. Figures (a) & (b) have the wine glass on the left while (c) accurately provides what the prompt is requesting.

5 Conclusion

In this work, we identify a key flaw (compute dumping) in the state-of-the-art test-time scaling algorithm [4] and propose the Verifier-Threshold algorithm as an effective solution. We demonstrate its performance and efficiency advantages across multiple verifiers on the GenEval benchmark. For future work, we plan to investigate adaptive verifier thresholds that vary across denoising steps and explore strategies to automate their selection. We also aim to extend our approach to standard diffusion models (beyond flow-based models).

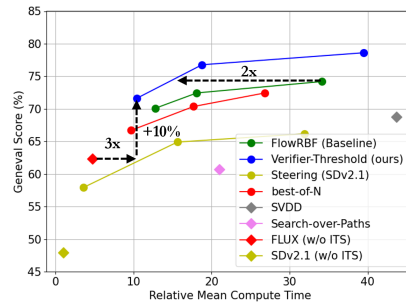


Figure 5: Test-time scaling when ImageReward [21] is used as verifier.

References

- [1] Dhruba Ghosh, Hannaneh Hajishirzi, and Ludwig Schmidt. Geneval: An object-focused framework for evaluating text-to-image alignment. *Advances in Neural Information Processing Systems*, 36:52132–52152, 2023.
- [2] Zhiqiu Lin, Deepak Pathak, Baiqi Li, Jiayao Li, Xide Xia, Graham Neubig, Pengchuan Zhang, and Deva Ramanan. Evaluating text-to-visual generation with image-to-text generation. In *European Conference on Computer Vision*, pages 366–384. Springer, 2024.
- [3] Black Forest Labs, Stephen Batifol, Andreas Blattmann, Frederic Boesel, Saksham Consul, Cyril Diagne, Tim Dockhorn, Jack English, Zion English, Patrick Esser, Sumith Kulal, Kyle Lacey, Yam Levi, Cheng Li, Dominik Lorenz, Jonas Müller, Dustin Podell, Robin Rombach, Harry Saini, Axel Sauer, and Luke Smith. Flux.1 kontext: Flow matching for in-context image generation and editing in latent space, 2025. URL <https://arxiv.org/abs/2506.15742>.
- [4] Jaihoon Kim, Taehoon Yoon, Jisung Hwang, and Minhyuk Sung. Inference-time scaling for flow models via stochastic generation and rollover budget forcing. *arXiv preprint arXiv:2503.19385*, 2025.
- [5] Google DeepMind. Nano banana: Gemini 2.5 flash image. [urlhttps://blog.google/products/gemini/updated-image-editing-model/](https://blog.google/products/gemini/updated-image-editing-model/), 2025. Image generation / editing model, announcement August 26, 2025.
- [6] OpenAI. Introducing our latest image generation model in the api. <https://openai.com/index/image-generation-api/>, April 2025. API access to gpt-image-1 (same image system as 4o in ChatGPT).
- [7] Apple Machine Learning Research. Univg: A generalist diffusion model for unified image generation and editing. <https://machinelearning.apple.com/research/univg-diffusion-model>, 2025. Apple ML Research page describing the UniVG image generation/editing model.
- [8] Midjourney. Version 7. <https://docs.midjourney.com/hc/en-us/articles/32199405667853-Version>, April 2025. V7 released Apr 3, 2025; default since Jun 17, 2025.
- [9] Stability AI. Introducing stable diffusion 3.5. <https://stability.ai/news/introducing-stable-diffusion-3-5>, October 2024. Launch post for SD 3.5 (Large / Large Turbo / Medium).
- [10] Kaiyi Huang, Kaiyue Sun, Enze Xie, Zhenguo Li, and Xihui Liu. T2i-compbench: A comprehensive benchmark for open-world compositional text-to-image generation. *Advances in Neural Information Processing Systems*, 36:78723–78747, 2023.
- [11] Charlie Snell, Jaehoon Lee, Kelvin Xu, and Aviral Kumar. Scaling llm test-time compute optimally can be more effective than scaling model parameters. *arXiv preprint arXiv:2408.03314*, 2024.
- [12] Daya Guo, Dejian Yang, Haowei Zhang, Junxiao Song, Ruoyu Zhang, Runxin Xu, Qihao Zhu, Shirong Ma, Peiyi Wang, Xiao Bi, et al. Deepseek-r1: Incentivizing reasoning capability in llms via reinforcement learning. *arXiv preprint arXiv:2501.12948*, 2025.
- [13] Nanye Ma, Shangyuan Tong, Haolin Jia, Hexiang Hu, Yu-Chuan Su, Mingda Zhang, Xuan Yang, Yandong Li, Tommi Jaakkola, Xuhui Jia, et al. Inference-time scaling for diffusion models beyond scaling denoising steps. *arXiv preprint arXiv:2501.09732*, 2025.
- [14] Le Zhuo, Liangbing Zhao, Sayak Paul, Yue Liao, Renrui Zhang, Yi Xin, Peng Gao, Mohamed Elhoseiny, and Hongsheng Li. From reflection to perfection: Scaling inference-time optimization for text-to-image diffusion models via reflection tuning. *arXiv preprint arXiv:2504.16080*, 2025.
- [15] Yunho Jin, Gu-Yeon Wei, and David Brooks. The energy cost of reasoning: Analyzing energy usage in llms with test-time compute. *arXiv preprint arXiv:2505.14733*, 2025.

- [16] Stelia. How reasoning ai models are transforming edge infrastructure, March 2025. URL <https://newsroom.stelia.ai/how-reasoning-ai-models-are-transforming-edge-infrastructure/>. Accessed: YYYY-MM-DD.
- [17] Prafulla Dhariwal and Alexander Nichol. Diffusion models beat gans on image synthesis. *Advances in neural information processing systems*, 34:8780–8794, 2021.
- [18] Jonathan Ho, Ajay Jain, and Pieter Abbeel. Denoising diffusion probabilistic models. *Advances in neural information processing systems*, 33:6840–6851, 2020.
- [19] Keyu Tian, Yi Jiang, Zehuan Yuan, Bingyue Peng, and Liwei Wang. Visual autoregressive modeling: Scalable image generation via next-scale prediction. *Advances in neural information processing systems*, 37:84839–84865, 2024.
- [20] Tim Salimans and Jonathan Ho. Progressive distillation for fast sampling of diffusion models. *arXiv preprint arXiv:2202.00512*, 2022.
- [21] Jiazheng Xu, Xiao Liu, Yuchen Wu, Yuxuan Tong, Qinkai Li, Ming Ding, Jie Tang, and Yuxiao Dong. Imagereward: Learning and evaluating human preferences for text-to-image generation. *Advances in Neural Information Processing Systems*, 36:15903–15935, 2023.
- [22] Alec Radford, Jong Wook Kim, Chris Hallacy, Aditya Ramesh, Gabriel Goh, Sandhini Agarwal, Girish Sastry, Amanda Askell, Pamela Mishkin, Jack Clark, et al. Learning transferable visual models from natural language supervision. In *International conference on machine learning*, pages 8748–8763. PmLR, 2021.
- [23] OpenAI. Learning to reason with llms. <https://openai.com/index/learning-to-reason-with-llms/>, 2024. Accessed: 2025-09-29.
- [24] Niklas Muennighoff, Zitong Yang, Weijia Shi, Xiang Lisa Li, Li Fei-Fei, Hannaneh Hajishirzi, Luke Zettlemoyer, Percy Liang, Emmanuel Candès, and Tatsunori Hashimoto. s1: Simple test-time scaling. *arXiv preprint arXiv:2501.19393*, 2025.
- [25] Xiner Li, Yulai Zhao, Chenyu Wang, Gabriele Scalia, Gokcen Eraslan, Surag Nair, Tommaso Biancalani, Shuiwang Ji, Aviv Regev, Sergey Levine, et al. Derivative-free guidance in continuous and discrete diffusion models with soft value-based decoding. *arXiv preprint arXiv:2408.08252*, 2024.
- [26] Raghav Singhal, Zachary Horvitz, Ryan Teehan, Mengye Ren, Zhou Yu, Kathleen McKeown, and Rajesh Ranganath. A general framework for inference-time scaling and steering of diffusion models. *arXiv preprint arXiv:2501.06848*, 2025.
- [27] Xiner Li, Yulai Zhao, Chenyu Wang, Gabriele Scalia, Gokcen Eraslan, Surag Nair, Tommaso Biancalani, Shuiwang Ji, Aviv Regev, Sergey Levine, et al. Derivative-free guidance in continuous and discrete diffusion models with soft value-based decoding. *arXiv preprint arXiv:2408.08252*, 2024.

A Experimental Setup

A.1 Dataset & Models

For evaluating our models we employ the widely-used GenEval dataset [1]. It contains 553 prompts which checks six different attributes: single object, two object, counting, colors, position, and attribute binding. For the generator, we use the FLUX-Schnell model [3] extensively due to its SOTA performance and baseline implementation from FlowRBF [4]. We run it consistently for ten denoising steps for best results. For the verifiers, we use ImageReward [21] and VQAScore [2] which are both variants of the CLIP model [22].

A.2 Methods

We use the same setup and hyperparameters as FlowRBF [4] for all the methods: Best-of- N , search-over-paths, SVDD, and FlowRBF itself. We use a verifier threshold value (Δ) of 0.005 and 0.00125 for ImageReward and VQAScore respectively when the total NFEs is 40. For subsequent total NFEs of 80 and 160, we correspondingly multiplied the threshold values with $2\times$, $4\times$ the above value.

B Related Work

Test-time compute as a new scaling axis

In recent years, scaling of AI models has mainly involved increasing model size and the amount of compute and data utilized during training. However, recent work shows that spending more compute at test-time can substantially improve output quality and reasoning capability, thus creating a new dimension for scaling compute to improve model performance. OpenAI’s o1 series popularized this paradigm by spending more test-time budget on deliberate “thinking” before answering [23]. DeepSeek-R1/R1-Zero similarly leverages extended reasoning trajectories at inference [12]. Snell et al. formalize when scaling test-time compute can be more effective than scaling model size [11]. Complementing these analyses, *s1* demonstrates a simple and effective test-time scaling recipe with strong empirical gains [24].

Test-time scaling for image generation

While diffusion models and flow models have achieved impressive results in image and video generation, naive generation with these models often fails to satisfy complex user instructions involving object quantities, relative position, and size, among other conceptual attributes. Recently, test-time scaling methods have been developed for diffusion and flow models that significantly outperform naive generation.

Reward-based sampling and noise-search

Reward-based sampling methods repeatedly sample from the model’s learned distribution, guided by a reward such as text–image alignment or aesthetic quality, to select higher-quality outputs. The most basic example is Best-of- N (BoN), which generates N independent images with different random seeds and picks the one with the highest reward. Ma et al. (2025) formalize this paradigm by introducing both **BoN** and Search-over-Paths (**SoP**), the latter refining trajectories by sampling particles along the denoising path [13]. Building on this idea, “noise trajectory search” methods incorporate reward-guided selection directly into the denoising process: **SVDD** [25] selects, at every denoising step, the particle with the highest expected reward. Extending reward-based search to flow models, Kim et al. (2025) [4] propose three complementary techniques: test-time SDE conversion, which introduces stochasticity into otherwise deterministic flows; interpolant conversion, which alters the trajectory interpolant to expand the search space; and Rollover Budget Forcing (**RBF**), which dynamically reallocates compute across timesteps by advancing any particle that exceeds the previous best reward and rolling over unused function evaluations to future steps, thereby ensuring efficient utilization of the total budget.

C Comprehensive Results

In this section, we flush out the plots in Fig. 1 & Fig. 5 in the form of Tab. 1. We also show the images generated for various example prompts, especially in cases where our approach succeeds when other baselines fail, and also some cases where all approaches fail. In all the example images, Fig. (a) corresponds to the image generated without test-time scaling, Fig. (b) corresponds to the one generated using FlowRBF [4] and Fig. (c) is the one generated by our Verifier-Threshold algorithm.

Method	Generator	Verifier	NFEs	time (\times)	GenEval (%)
Regular-T2I	SDv2.1	-	1	1	47.93
Regular-T2I	FLUX-Schnell	-	10	4.74	62.33
Steering [26]	SDv2.1	ImageReward [21]	4	3.57	57.93
Steering [26]	SDv2.1	ImageReward [21]	20	15.62	64.91
Steering [26]	SDv2.1	ImageReward [21]	40	31.91	66.18
BoN [13]	FLUX-Schnell	ImageReward [21]	40	9.70	70.62
BoN [13]	FLUX-Schnell	ImageReward [21]	80	17.16	70.36
BoN [13]	FLUX-Schnell	ImageReward [21]	160	26.39	72.45
BoN [13]	FLUX-Schnell	VQAScore [2]	40	10.29	70.07
BoN [13]	FLUX-Schnell	VQAScore [2]	80	18.72	70.54
BoN [13]	FLUX-Schnell	VQAScore [2]	160	27.07	71.91
SoP [13]	FLUX-Schnell	ImageReward [21]	250	21.00	60.68
SoP [13]	FLUX-Schnell	VQAScore [2]	250	22.25	61.19
SVDD [27]	FLUX-Schnell	ImageReward [21]	250	43.69	68.76
SVDD [27]	FLUX-Schnell	VQAScore [2]	250	56.74	72.89
FlowRBF [4]	FLUX-Schnell	ImageReward [21]	40	12.80	70.10
FlowRBF [4]	FLUX-Schnell	ImageReward [21]	80	18.11	72.45
FlowRBF [4]	FLUX-Schnell	ImageReward [21]	160	34.11	74.20
FlowRBF [4]	FLUX-Schnell	VQAScore [2]	40	13.83	70.32
FlowRBF [4]	FLUX-Schnell	VQAScore [2]	80	27.03	71.77
FlowRBF [4]	FLUX-Schnell	VQAScore [2]	160	48.98	73.45
VT (Ours)	FLUX-Schnell	ImageReward [21]	40	10.31	71.61
VT (Ours)	FLUX-Schnell	ImageReward [21]	80	18.68	76.77
VT (Ours)	FLUX-Schnell	ImageReward [21]	160	39.36	78.62
VT (Ours)	FLUX-Schnell	VQAScore [2]	40	12.80	73.83
VT (Ours)	FLUX-Schnell	VQAScore [2]	80	25.90	76.12
VT (Ours)	FLUX-Schnell	VQAScore [2]	160	51.97	77.20

Table 1: Comparison of different approaches across models, verifiers, NFEs, along with their efficiency (wall-clock time) & performance (GenEval) scores. Methods are Best-of- N (BoN), Search-over-Paths (SoP), Soft Value-based Decoding in Diffusion (SVDD), and Verifier-Threshold (VT).



Figure 7: “a photo of a purple wine glass and a black apple”. For all examples in this section, Fig. (a) is the image generated without test-time scaling, Fig. (b) is generated using FlowRBF [4] and Fig. (c) is generated by our Verifier-Threshold algorithm.



(a)



(b)



(c)

Figure 8: “a photo of four clocks”



(a)



(b)



(c)

Figure 9: “a photo of a bench left of a bear”



(a)



(b)



(c)

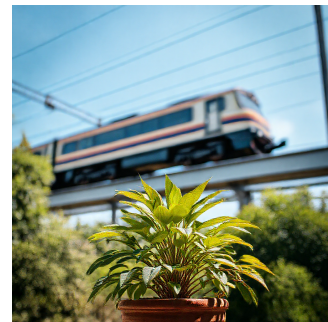
Figure 10: “a photo of three sports balls”



(a)



(b)



(c)

Figure 11: “a photo of a train above a potted plant”



(a)



(b)



(c)

Figure 12: “a photo of a brown oven and a purple train”



(a)



(b)



(c)

Figure 13: “a photo of a purple carrot”



(a)

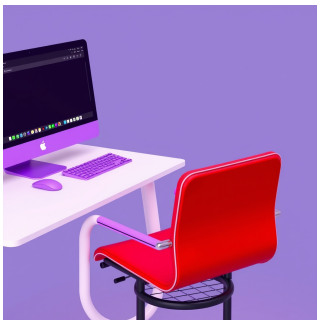


(b)



(c)

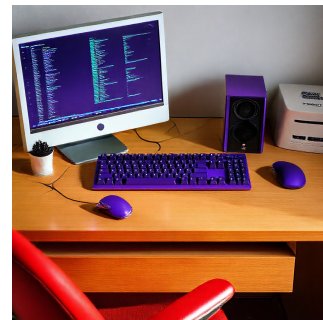
Figure 14: “a photo of a wine glass right of a hot dog”



(a)

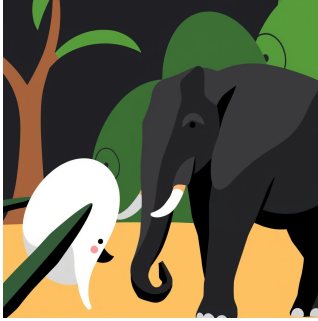


(b)



(c)

Figure 15: “a photo of a purple computer keyboard and a red chair”



(a)



(b)



(c)

Figure 16: “a photo of a white banana and a black elephant”



(a)



(b)



(c)

Figure 17: “a photo of an orange handbag and a green carrot”



(a)



(b)



(c)

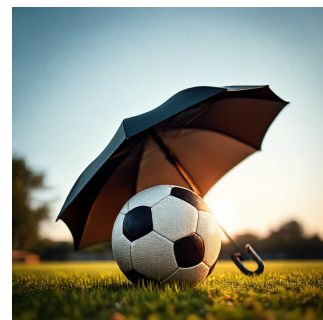
Figure 18: “a photo of an orange donut and a yellow stop sign”



(a)



(b)



(c)

Figure 19: “a photo of a sports ball left of an umbrella”